


Article

Sustainable Use of Marine Macroalga *Sargassum muticum* as a Biosorbent for Hazardous Crystal Violet Dye: Isotherm, Kinetic and Thermodynamic Modeling

Mustafa A. Fawzy ^{1,2}, Abeer S. Aloufi ³, Sedky H. A. Hassan ^{4,*}, Abdulrahman H. Alessa ⁵, Ahmad A. Alsaigh ⁶, Mostafa Koutb ⁶ and Ismail R. Abdel-Rahim ¹

¹ Botany and Microbiology Department, Faculty of Science, Assiut University, Assiut 71516, Egypt; mustafa.fawzy@aun.edu.eg or mafawzy@tu.edu.sa (M.A.F.); ismailramadan@aun.edu.eg (I.R.A.-R.)

² Biology Department, Faculty of Science, Taif University, P.O. Box 11099, Taif 21944, Saudi Arabia

³ Department of Biology, College of Science, Princess Nourah bint Abdulrahman University, P.O. Box 84428, Riyadh 11671, Saudi Arabia; asaloufi@pnu.edu.sa

⁴ Department of Biology, College of Science, Sultan Qaboos University, Muscat 123, Oman

⁵ Department of Biology, Faculty of Science, University of Tabuk, Tabuk 47512, Saudi Arabia; alessiabdulrahman@gmail.com

⁶ Department of Biology, Faculty of Science, Umm Al-Qura University, Makkah 24381, Saudi Arabia; aassaigh@uqu.edu.sa (A.A.A.); mmkoutb@uqu.edu.sa (M.K.)

* Correspondence: s.hassan@squ.edu.om; Tel.: +968-93879120

Abstract: The pollution of aquatic bodies by synthetic dyes is regarded as one of the most significant environmental issues, which has prompted greater research into effective and sustainable removal techniques. Even though there have been major efforts in the previous few decades, more study is still necessary to fully examine the long-term performance and usable applicability of adsorbents and different adsorption techniques for the removal of dye. In the present study, a brown marine macroalga *Sargassum muticum* was used as an effective and sustainable biosorbent for the crystal violet (CV) dye removal from aqueous solutions. The biosorbent was characterized by analysis of SEM, EDX, and FTIR. In order to evaluate the optimum conditions of CV biosorption, several parameters have been examined as a function of contact time, algal dose, initial concentration of CV, and pH. The maximum CV removal was obtained at 60 min contact time, 10 g/L algal dosage, 30 mg/L initial concentration of CV, and pH 6. The isothermal models of Langmuir, Freundlich, Dubinin-Radushkevich, and Temkin are best explained the equilibrium data obtained. At the optimum conditions, the maximum biosorption capacity of the algal biomass achieved from the Langmuir model was 39.1 mg/g. The kinetic adsorption models were also better explained using the pseudo-second-order and Elovich model, and the effect of the boundary layer was indicated using the intraparticle diffusion model as well as the chemisorption-controlled biosorption process. Thermodynamically, the process of CV biosorption was shown to be random, spontaneous, and endothermic. Furthermore, the proposed mechanism of CV dye biosorption onto algal biomass is regulated by hydrogen bond formation, electrostatic interaction, and ion exchange. These findings revealed that the biomass of *S. muticum* is a sustainable and promising material for the biosorption of water pollutants.

Keywords: biosorption; crystal violet; kinetics and isothermal studies; *Sargassum muticum*; thermodynamic analysis



Citation: Fawzy, M.A.; Aloufi, A.S.; Hassan, S.H.A.; Alessa, A.H.; Alsaigh, A.A.; Koutb, M.; Abdel-Rahim, I.R. Sustainable Use of Marine Macroalga *Sargassum muticum* as a Biosorbent for Hazardous Crystal Violet Dye: Isotherm, Kinetic and Thermodynamic Modeling. *Sustainability* **2023**, *15*, 15064. <https://doi.org/10.3390/su152015064>

Academic Editor: Agostina Chiavola

Received: 8 September 2023

Revised: 9 October 2023

Accepted: 11 October 2023

Published: 19 October 2023



Copyright: © 2023 by the authors. Licensee MDPI, Basel, Switzerland. This article is an open access article distributed under the terms and conditions of the Creative Commons Attribution (CC BY) license (<https://creativecommons.org/licenses/by/4.0/>).

1. Introduction

The contamination of aquatic ecosystems by synthetic dyes is considered to be one of the most important environmental problems since dye-containing effluents from different industries such as cosmetics, paper, plastics and textiles are constantly discharged into the sea or the rivers [1,2]. On the other hand, due to their teratogenic, mutagenic, and

carcinogenic properties, the non-biodegradable origin of dyes poses a significant danger to human health and to marine biota [3]. In addition, the presence of dyes in the aquatic ecosystem leads to a high decrease in the penetration of light and the quantity of oxygen dissolved in water, resulting in further harmful effects on the photosynthetic activity of plants [4]. The toxicological impact resulting from the release of dye effluents into the aquatic environment is, therefore, a relevant issue worldwide.

Crystal violet is a synthetic and cationic dye used as a purple dye in several industries and a pH indicator, as well as in the Gram method to stain bacteria, as a bacteriostatic agent, and in different medical fields [5]. It could cause extreme inflammation of the eyes and renal failure that leads to cancer and permanent blindness [6]. The dye remediation from wastewater has, therefore, become important for the environment, and various methods are used for dye removal, such as membrane filtration, reverse osmosis, chemical oxidation, flocculation, coagulation, precipitation and photodegradation [7–9]. These processes, however, have some drawbacks, such as difficulties in efficiently disposing of dye wastewater, high energy consumption, or high costs [10].

The biosorption process by low-cost biosorbent provides an appealing and sustainable method for dye removal. It involves physicochemical removal mechanisms such as chelation, microprecipitation, complexation, ion exchange, and adsorption [11]. The biosorbent can be used in the sorption method in living and non-living forms; the latter is more favorable and realistic since the toxicity of dye molecules does not affect them. There are numerous materials such as cotton waste [12], rice husks [13], algae [14], chitosan [15], fungi [16], and plants [17] have been used for dye removal from wastewater. Algae have been shown to be a possible material for dye adsorption among these materials due to their availability, low cost, and widespread appearance in nature.

In recent years, researchers have drawn considerable interest to the uniqueness of marine macroalgae as a renewable biosorbent [18,19]. These marine macroalgae are present in abundance in several areas around the world. The high binding affinity as well as high surface area and the existence of a specific chemical composition of these marine macroalgae have become the essential features for them to become strong biosorbent. Furthermore, marine macroalgae have rapid biosorption ability, with high uptake efficiency, whereas the chief constituent of marine macroalgae is polysaccharide, which consists of polycolloid, carrageenan, and alginate that are capable of binding surface contaminants [20]. In addition to the other functional groups, such as amine, carbonyl, carboxyl and hydroxyl; alginate and sulfate are the primary active groups in brown macroalgae, which play a crucial role in the water pollutants adsorption [21]. Previous investigations have shown that brown macroalgae *Laminaria japonica* [22], *Nizamuddina zanardini* [23] and *Sargassum hemiphyllum* [24] have been found to be possibly suitable biosorbents with high removal rates of dyes. The ability of biosorption depends on the sorbate and biosorbent, as well as many factors, such as initial ion concentration, contact time and pH of the solution [25].

The purpose of this work is to investigate the efficacy of marine brown macroalgae *Sargassum muticum* for crystal violet dye removal from the aqueous solutions under various conditions, such as biosorption time, biosorbent dosage, initial dye concentrations, and pH. Moreover, kinetic, isothermal, and thermodynamics studies of biosorption have been investigated. Finally, the performance of the *S. muticum* biomass was also studied for the removal of crystal violet dye from real wastewater.

2. Materials and Methods

2.1. Collection and Preparation of Algae

Marine brown macroalga *Sargassum muticum* (Yendo) Fensholt was handily collected from the coastal region of Jeddah (Red Sea), Saudi Arabia, at a depth of 0.3 m. The samples of algae were taken to the laboratory, washed with tap water for removal of suspended epiphytes, salts, and other contaminants, washed again with deionized water, and then dried for 24 h at 60 °C. With a mortar, the dry samples were ground and sieved using a 1.0 mm sieve. Every 1 g of powdered sample was added to 100 mL of 0.2% CaCl₂ to

improve the biomass sorption potential. The samples were then cleaned several times with deionized water, dried up to constant weight at 50 °C, and stored at room temperature [1].

2.2. Adsorbate Solution

Crystal Violet dye solutions (CV; molecular formula $C_{25}H_{30}N_3Cl$; Figure 1) were prepared using deionized water by diluting the CV dye stock solution (1000 mg/L). The reagents obtained from Sigma-Aldrich and used as provided, such as CV dye, HCl, NaOH, and $CaCl_2$, are of analytical grade.

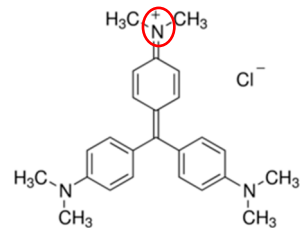


Figure 1. Molecular structure of Crystal violet. Red circle is the active site.

2.3. Biosorption Experiments

The experiments of CV dye biosorption were done in 250 mL conical flasks containing 100 mL of CV dye solution. To optimize the experimental conditions, the impacts of contact time of 0–150 min, algal dosage of 2–10 g/L, initial CV dye concentrations of 10–90 mg/L, and pH of 2–10 were investigated, and pH of the solutions was adjusted by 0.1 M NaOH and 0.1 M HCl. The samples were shaken at 170 rpm in a shaker at 25 °C, the samples were filtered, and the CV dye concentrations were determined using a UV-vis spectrometer (Unico UV-2100; USA) with a 590 nm wavelength using a calibration curve. All the experiments were performed in triplicates.

The data obtained were evaluated for the estimation of the CV dye kinetic model at different time intervals and for determining the isothermal adsorption model at different initial dye concentrations. Thermodynamic analyses of biosorption of CV dye and the effect of temperature have also been studied by testing the process of biosorption under optimized conditions at various temperatures (25, 35, and 45 °C).

Using Equation (1), the amount of CV molecules biosorbed per biosorbent mass unit was calculated. The percentage of adsorbed CV by *S. muticum* biomass has been estimated by Equation (2):

$$q_e = \frac{V (C_i - C_{eq})}{W} \quad (1)$$

$$Removal (\%) = \frac{(C_i - C_{eq})}{C_i} \times 100 \quad (2)$$

where q_e (mg/g) is the CV dye concentration adsorbed per unit mass, C_i and C_{eq} (mg/L) are the concentration of CV dye before and after the process of sorption, respectively, W (g) is the biosorbent amount, and V (L): the solution volume.

2.4. Characterization of Algal Biomass

2.4.1. Scanning Electron Microscopy and Energy Dispersive Spectroscopy

Using a scanning electron microscope (SEM, JSM-6510 LV (JEOL; USA)) combined with energy-dispersive X-ray (EDX, JEOL JEM-2100 (USA)), the algal biomass was analyzed before and after dye treatment.

2.4.2. Fourier Transform Infrared Spectra (FTIR)

The FTIR for optimized algal biomass was recorded on the Nicolet IS 10 FTIR spectrometer.

2.5. Statistical Analysis

All experiments in this study were performed in triplicate, and the data were displayed as mean ± standard error (SE). The SPSS software (version 16.0, Chicago, IL, USA) was used to compare the means using Duncan’s multiple range tests.

3. Results and Discussion

3.1. Biosorbent Characterization

3.1.1. SEM

Scanning electron micrograph (SEM) has been used before and after the dye biosorption to study the distribution of CV ions on the *S. muticum* surface (Figure 2A,B). Algal cells were smooth with a surface greatly porous, which was hole-like prior to CV dye exposure (Figure 2A). The algal surface became meandrous and rough after treatment with CV dye (Figure 2B). This is attributed to the dye ions accumulation along the algal cell surface. The algal cell wall was very porous and readily permeable to CV ions. This can clarify the greatest affinity of *S. muticum* biomass for the CV dye removal. Changes in the algal surface porosity related to the biosorption of dyes were reported by Omar et al. [26] and Vijayaraghavana and Shanthakumarb [27].

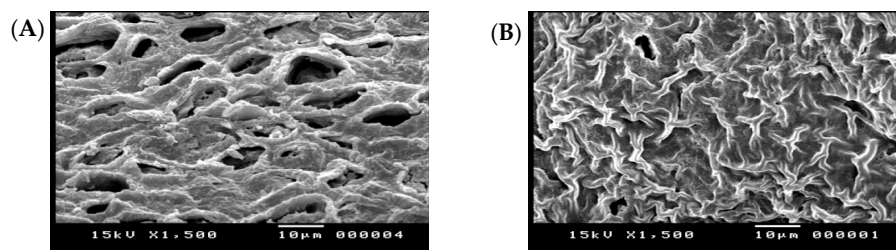


Figure 2. SEM of the *S. muticum* biomass (A) before and (B) after the CV biosorption.

3.1.2. Energy Dispersive Spectroscopy (EDX)

The elemental compositions of *S. muticum* biomass before and after CV biosorption were determined using an EDX analysis (Figure 3A,B). The data showed that carbon and oxygen were found to be the most abundant elements found in the algal biomass prior to dye biosorption, followed by calcium and, ultimately, magnesium, silicon, sulfur, and aluminum (Figure 3A). The increase in carbon weight percentage from 27.21% (before dye biosorption) to 32.11% (after biosorption) and the presence of chlorine element as a constituent of the dye structure after biosorption may be responsible for the biosorption of CV by algal biomass. Moreover, some elements in the spectrum were undetectable or reduced during dye biosorption, indicating that the process responsible for the biosorption of CV dye is ion exchange [1].

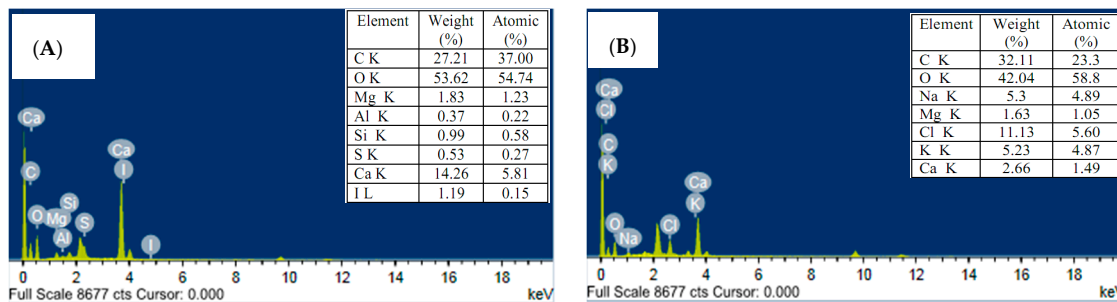


Figure 3. EDX of the *S. muticum* biomass (A) before and (B) after the CV biosorption.

3.1.3. FTIR Analysis

The spectrum of FT-IR of *S. muticum* biomass before and after biosorption of CV dye includes peaks distinguished by numerous functional groups (Figure 4A,B). The wide

peak at 3416 cm^{-1} was recorded before and after biosorption of CV onto the algal biomass due to groups of $-\text{NH}$ and $-\text{OH}$. This suggests that the biosorption of CV dye onto the *S. muticum* biomass is the responsibility of the hydroxyl and amine groups [18]. Intense peaks allocated to the $\text{C}-\text{H}$ group of phospholipids and lipid fractions were observed on the biomass of *S. muticum* at 2925.35 cm^{-1} and 2924.78 cm^{-1} before and after biosorption of CV dye [28]. The absorption band of 1632.57 cm^{-1} transferred to 1635.66 cm^{-1} may be assigned to the $\text{C}=\text{O}$ stretching vibration of alginic acid on the brown algae cell wall [29]. In addition, typical peaks at 1424 cm^{-1} and 1034 cm^{-1} belonging to alginate component were recorded for the biomass of *S. muticum* before and after the biosorption process, along with a new lipid peak containing the fraction of fucoïdan (sulfated polysaccharides) was occurred at 1260.30 cm^{-1} for the algal biomass after treatment with CV dye, previously mentioned in the study of Pennesi et al. [30] and Marais and Joseleau [31]. As proposed by Kumar and Ahmad [32], the presence of a new absorption band at 1540.66 cm^{-1} in the *S. muticum* biomass may be due to the $-\text{CN}$ group of the CV after biosorption. The peaks present only in the algal biomass at 584.22 cm^{-1} and 594.16 cm^{-1} after biosorption process may be attributed to the $\text{C}-\text{H}$ stretching vibration [33]. According to the analysis of FTIR spectra, shifts in the functional groups' position in the biomass of *S. muticum* after CV biosorption suggest that these groups are active in the removal of CV. A high quantity of polysaccharides is found on the surface of the algal cell; some of them are linked to proteins and other molecules [34]. These components have many active functional groups, such as sulfate, phosphate, amino, carboxyl, amine, and carbonyl groups [35]. The CV dye molecules were, therefore, incorporated with the algal biomass by association with the functional groups, as suggested by Jayaraj et al. [36].

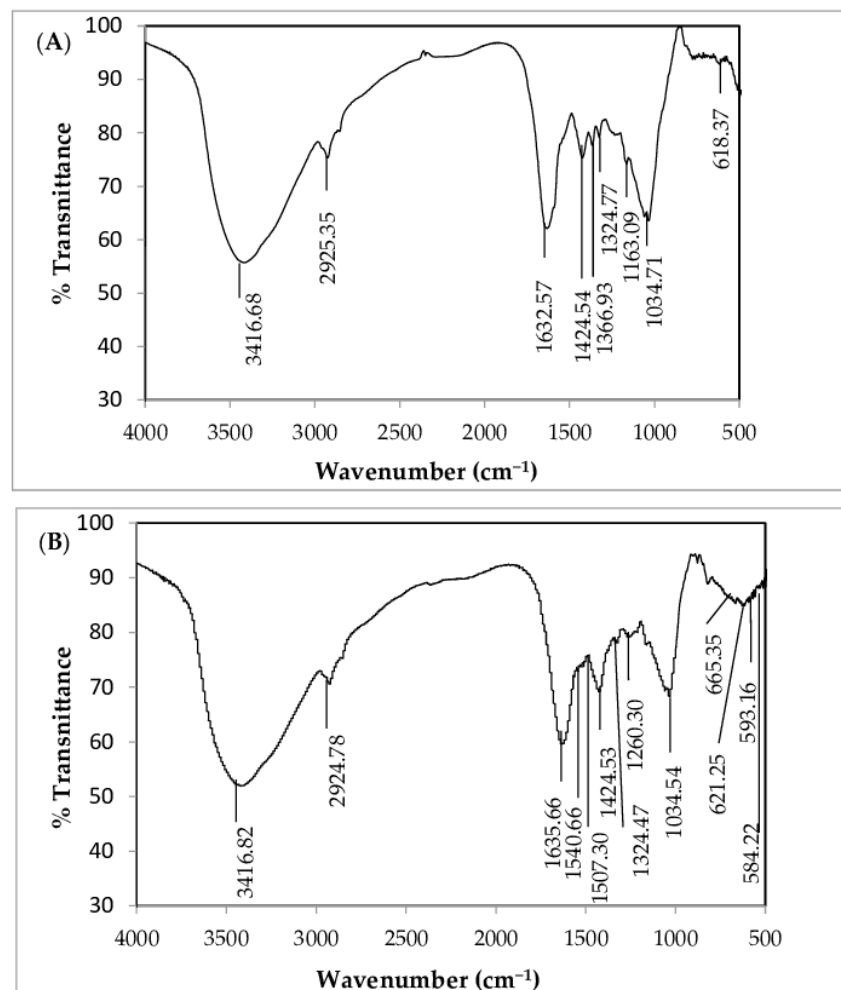


Figure 4. FTIR spectrum of the *S. muticum* biomass (A) before and (B) after the CV biosorption process.

3.2. Optimization of CV Biosorption Parameters

The optimization of different variables such as contact time, algal dose, initial concentrations of CV dye, and pH values was done at 25 °C for studying the CV biosorption onto *S. muticum* biomass.

3.2.1. Influence of Contact Time

The influence of contact time (0–150 min) on the removal of CV onto the biomass of *S. muticum* at constant conditions of 10 g/L algal dose, 50 mg/L initial concentration of CV, and pH 5 was investigated (Figure 5A). It could be noticed that CV dye biosorption is relatively rapid. The biosorption rose very rapidly in the first 40 min, then achieved equilibrium after 60 min and ultimately approached a constant at 60–150 min. The contact time was thus determined at 60 min as the optimum contact time, and the highest CV removal percentage at this time was 98.01%. These findings agree with the results of Aditiya and Al Kausar [37], who found that methylene blue and crystal violet dye biosorption onto *Spirulina* sp. biomass increased rapidly within the first 30 min and reached equilibrium at 60 min. On the other hand, Daneshvar et al. [38] found that dye removal by marine brown macroalgae increased rapidly within the first 10 min and reached equilibrium at 90 min. The disparity in removal rates of dyes among the algal biomasses could be attributed to variations in the composition and characteristics of the algal cell wall, surface charge density, and surface area [39]. At the outset, great numbers of the available free sites on the algal surface were definitely responsible for the high rate of CV biosorption, whereas the subsequent deceleration was found as the available free sites were saturated [23].

3.2.2. Influence of Algal Dosage

Figure 5B indicates the influence of the algal dose (2, 4, 6, 8, and 10 g/L) on the CV removal at an optimized contact time (60 min), as well as a fixed initial concentration of CV (50 mg/L) and pH 5. As the algal dosage increased, the efficiency of CV removal increased, and the highest removal of CV was 94.9% at an algal dose of 10 g/L. Similar results were observed with the biosorption of MB by *Sargassum hemiphyllum* [24]. The high removal efficiency could be due to the increased biosorption sites available with the high dose of biosorbent [40].

3.2.3. Influence of Initial Concentrations of CV Dye

Under optimal conditions of 60 min contact time, 10 g/L of biosorbent dosage, and fixed pH 5, the influence of initial CV concentrations (30–90 mg/L) on the removal percentage of CV (%) and CV biosorption capacity (q_e mg g⁻¹) by *S. muticum* biomass was assessed as indicated in Figure 5C,D. With a rise in the initial concentration of the CV, the dye removal percentage decreased (Figure 5C). The highest removal percentage of CV by *S. muticum* biomass was 94.6% at 30 mg/L of CV dye concentration. The reduction in the CV removal percentage can be due to the absence of adequate free-binding sites for the biosorption of CV. All the CV molecules in the aquatic solution may be associated with the free binding sites at lower concentrations, and so the percentage of CV removal was higher than those at higher concentrations of CV dye. On the other hand, the biosorption capacity (mg g⁻¹) increased by raising dye concentration due to the rise in driving force generated by the rising concentration gradient (Figure 5D). This minimizes any mass transfer resistances between CV dye molecules, increasing the biosorption capacity [41]. Furthermore, the increment in driving force speeds up the possibility of dye molecules colliding with the biosorbent, which raises the biosorption capacity of CV dye [42].

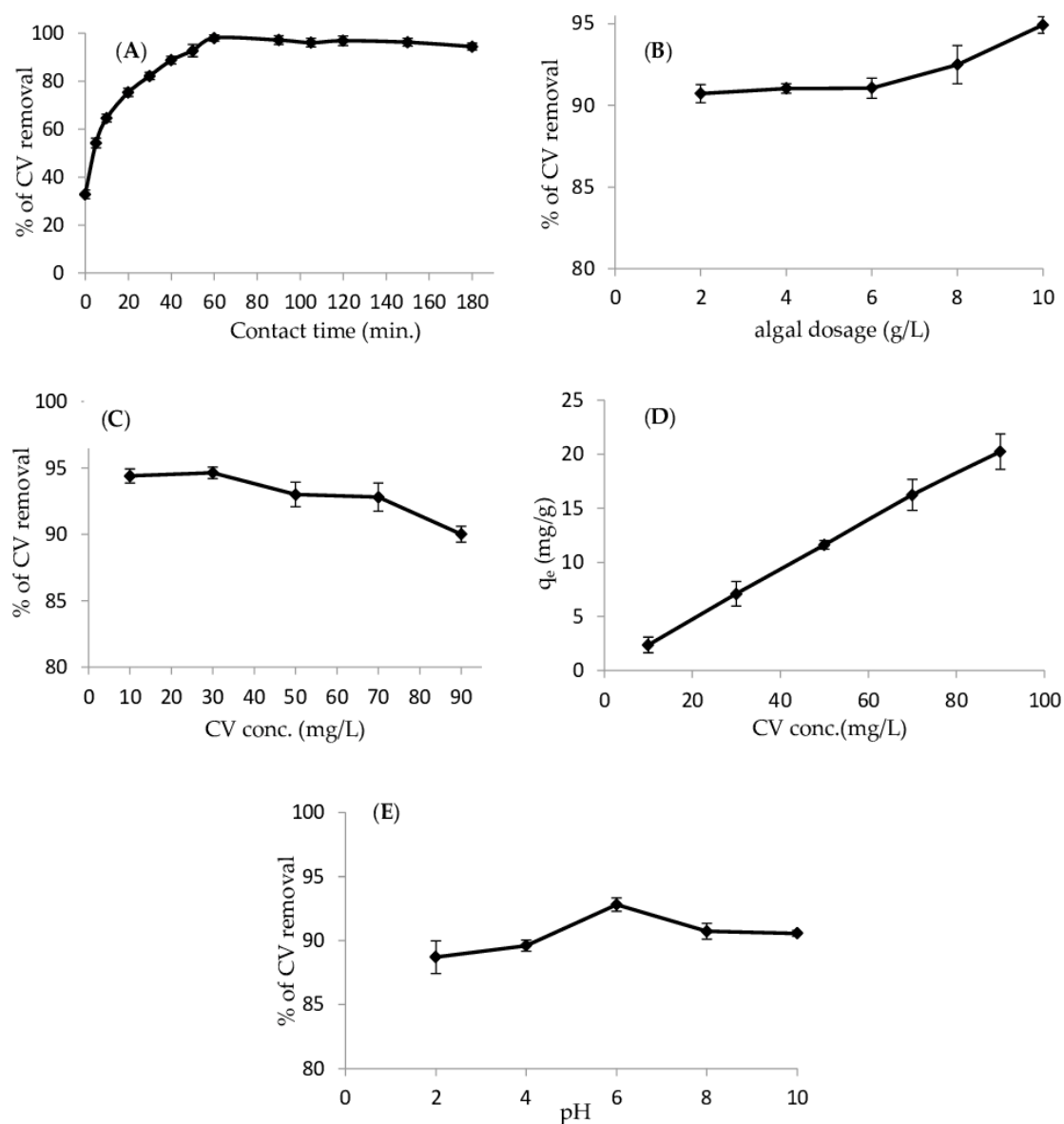


Figure 5. Influence of (A) Contact time, (B) Algal dose, (C) Initial conc. of CV, (D) Adsorption capacity, and (E) pH on the biosorption process of CV onto the *S. muticum* biomass.

3.2.4. Influence of pH Values

The influence of different pH (2–10) on the removal of CV under the optimum conditions of contact time (60 min), algal dose (10 g/L), and initial concentration of CV (30 mg/L) was investigated. Figure 5E indicates a rise in biosorption of CV with an increase in pH to the optimum value of pH 6 (92.8%), after which a small decrease in the CV biosorption rate was found. The dye of CV is a cation-based coloring agent, while the *S. muticum* cell wall consists predominantly of fucan, alginate, and proteins containing various negatively charged functional groups, such as hydroxyl, amine, sulfate, and carboxyl [43]. The surface charge of a biosorbent can change when the pH changes. Thus, the algal biomass's point of zero charge (pH_{ZPC}) was evaluated according to the method of Rivera-Utrilla et al. [44] (The details are shown in Supplementary Materials). The biomass of *S. muticum* was found to have a pH_{ZPC} of about 5.6 (Figure S1). This shows that above this pH ($\text{pH} > \text{pH}_{\text{ZPC}}$), a negative charge occurs on the biomass surface due to the deprotonation of functional groups such as amino, hydroxyl, carboxyl, and sulfate, which increases the capability of CV biosorption by electrostatic attractions [45]. Nevertheless, below this pH ($\text{pH} < \text{pH}_{\text{ZPC}}$), the

algal biomass acquires a positive charge because of the protonation of functional groups, inducing hydrogen ions for competition with the cations of CV dye, causing a reduction in biosorption of dye. Despite this, CV dye still adsorbs, showing that dye biosorption is not solely caused by electrostatic interaction. The active binding sites, however, were limited; hence, the percentage of CV removal was not consistently raised as the pH was higher (>6).

3.3. Biosorption Kinetics

The data of biosorption kinetics provide useful knowledge about the reaction rate of a given system and allow for assessing the efficiency of the biosorbent and the process of adsorption underlying it. Biosorption kinetic studies are therefore important in order to well understand the process of biosorption. For this purpose, pseudo-first order [46], pseudo-second-order [47], Elovich [48], and intraparticle diffusion [49] have been used, and their equations are provided below:

$$\text{Pseudo-first order model: } \text{Log}(q_e - q_t) = \text{Log } q_e - \frac{K_1 t}{2.303} \quad (3)$$

$$\text{Pseudo-second order model: } \frac{t}{q_t} = \frac{1}{K_2 q_e^2} + \frac{t}{q_e} \quad (4)$$

$$\text{Elovich model: } q_t = \frac{1}{\beta} \ln(\alpha\beta) + \frac{1}{\beta} \ln(t) \quad (5)$$

$$\text{Intraparticle diffusion model: } q_t = K_i t^{1/2} + C_i \quad (6)$$

where q_e and q_t (mg/g) are the adsorbed quantity of CV dye at equilibrium and at any time (t). K_1 , K_2 , and K_i : the pseudo-first order, pseudo-second order, and Intraparticle diffusion rate constants, respectively. β (g/mg) and α (mg/g min): the surface coverage and initial rate constant of the Elovich model, respectively. Figure 6A–D displays the linear plots of $\log(q_e - q_t)$ vs. t , t/q_t vs. t , q_t vs. $t^{0.5}$, and q_t vs. $\ln t$, respectively, and has been used for verifying the model validity and for determining the model parameters (Table 1).

As seen in Figure 6A and Table 1, the high coefficient of determination value ($R^2 = 0.988$) shows that the pseudo-first-order model supports the experimental data of CV biosorption kinetics. However, the experimental q_e value (12.26 mg/g) is higher than the calculated value (7.39 mg/g). Thus, the pseudo-first-order model might not be appropriate to illustrate the CV dye biosorption onto the biomass of *S. muticum*. On the contrary, Fawzy and Gomaa [50] reported that the pseudo-first-order model was fit implemented for estimating the biosorption behaviors of Congo red dye onto the *Cystoseira trinodis* biomass.

The value of the determination coefficient (R^2) achieved by the pseudo-second-order model was 0.992 (Figure 6B; Table 1). In addition, the value of calculated q_e (12.55 mg/g) was close to the value of experimental q_e (12.26 mg/g), revealing that the kinetic model of pseudo-second order was a satisfactory way of explaining the CV biosorption onto *S. muticum*. The pseudo-second-order rate constant (K_2) for CV dye was 0.047 min^{-1} (Table 1), which promotes the more appropriate and rapid CV molecules biosorption by the biomass of *S. muticum* from aqueous solution. It was therefore suggested that the model of pseudo-second order is more fitting than the pseudo-first-order model for describing the CV biosorption onto the biomass of *S. muticum*, and the chemisorption controlled the biosorption process. These results were in agreement with the findings of Liang et al. [24], who indicated that the methylene blue biosorption onto *Sargassum hemiphyllum* biomass was followed by the pseudo-second order.

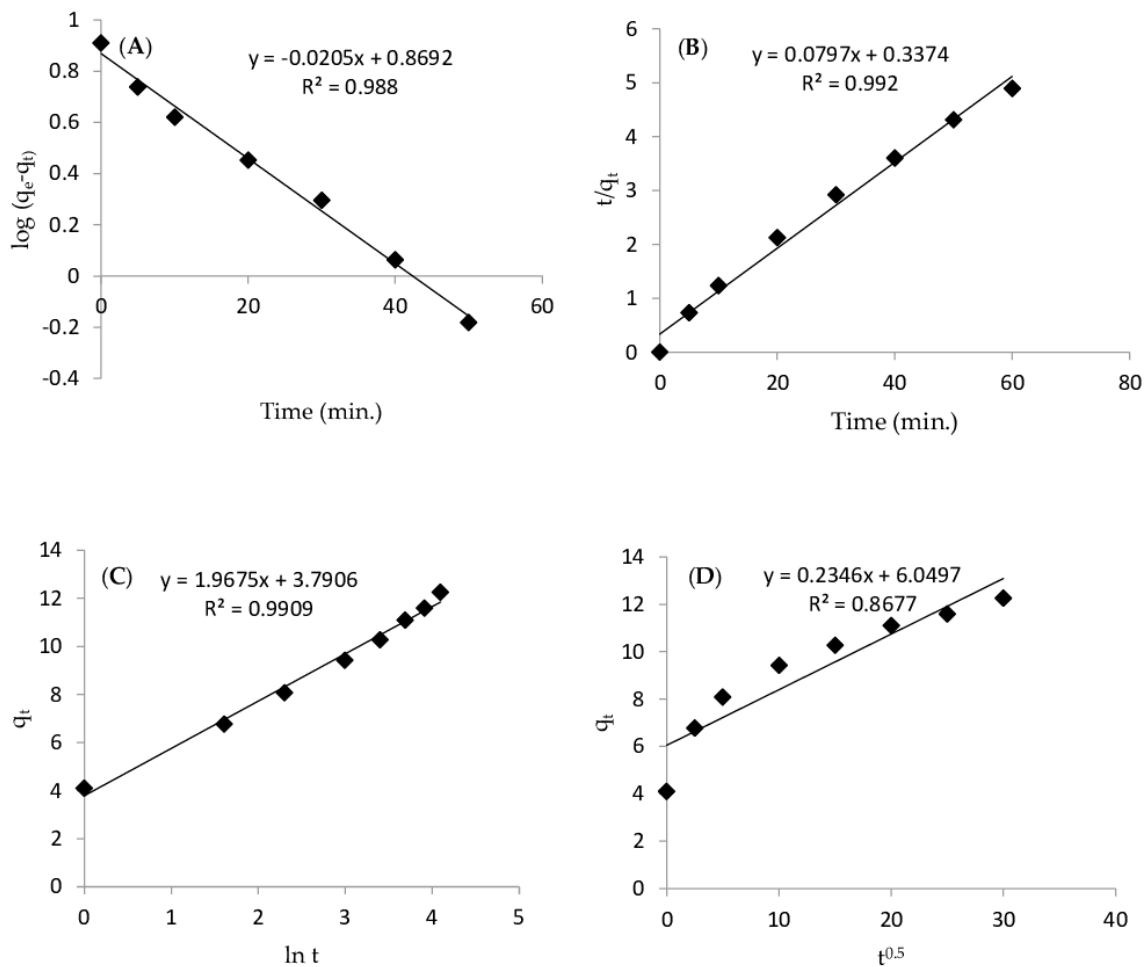


Figure 6. The linearization of (A) Pseudo-first order, (B) Pseudo-second order, (C) Elovich, and (D) Intraparticle diffusion kinetic models for the CV biosorption by *S. muticum* biomass.

Table 1. Sorption kinetic parameters obtained by CV biosorption onto *S. muticum*.

Kinetics Model	Parameters	Values
Pseudo-first order	q_e (exp.) (mg/g)	12.26
	q_e (cal.) (mg/g)	7.39
	K_1 (min^{-1})	0.047
	R^2	0.988
Pseudo-second order	q_e (cal.) (mg/g)	12.55
	K_2 (g/mg min)	0.02
	R^2	0.992
Elovich	α (g/mg min)	17.3
	β (g/mg)	0.508
	R^2	0.991
Intra-particle diffusion	K_i (mg/g $\text{min}^{0.5}$)	0.235
	C_i (mg/g)	6.05
	R^2	0.867

In order to analyze the CV biosorption process, more kinetic data were fitted to the Elovich kinetic model (Figure 6C). This model proposes that the active sites of biosorbents are heterogeneous and, hence, have different energies of sorption [51]. The high coefficient of determination value ($R^2 = 0.991$) shows that the experimental results were fitted by the Elovich kinetic model. The data in Table 1 indicated that α and β

constant values (17.3 g/mg min and 0.508 g/mg, respectively) were high, proposing that more biosorption sites are available on the biomass of *S. muticum* for CV dye biosorption.

The model of intraparticle diffusion is depicted in Figure 6D, which displays a linear relationship between the q_t against $t^{1/2}$. From Figure 6D, it is clear that the kinetic results are not well associated with the model of intraparticle diffusion because the linear plot does not pass through the origin (i.e., it is not the rate-limiting step) [49]. Furthermore, the low value of the determination coefficient (0.867) also showed that the model of intraparticle was not sufficiently suited for CV dye removal by *S. muticum*. The high intercept value (C_i , 6.05 mg/g; Table 1) may be clarified that a high number of smaller particles produced a greater surface area for removal of CV dye onto the algal biomass and a greater surface for biosorption process and thereby improved the effect of boundary layer [52].

3.4. Isothermal Biosorption Study

Different concentrations of initial CV dye (10, 30, 50, 70, and 90 mg/L) were used in the biosorption isothermal assay under previously optimized conditions (60 min contact time, 10 g/L algal dose, and pH of 6) at 25 °C.

In order to comprehend the mode of interaction between the biosorbent and CV dye, the isothermal models, as well as biosorption parameters determined according to the linearized isotherm forms for the models of the Langmuir, Freundlich, Temkin, and Dubinin–Radushkevich (D–R) are essential. Table 2 includes the isothermal parameters calculated from the linearized plots of the isotherm.

Table 2. Isotherm parameters for the CV biosorption onto the *S. muticum* biomass.

Isotherms	Parameters	Values
Langmuir	q_{max} (mg/g)	39.1
	b (L/mg)	0.12
	R_L	0.09–0.33
	R^2	0.954
Freundlich	n	1.27
	K_f (mg/g)	4.21
	R^2	0.977
	B	6.49
Temkin	A (L/mg)	2.18
	b (J/mol)	381
	R^2	0.970
Dubinin and Radushkevich	q_o (mg/g)	15.3
	$\beta \times 10^{-7}$ (mol ² /J ²)	3.0
	E (kJ/mol)	12.9
	R^2	0.915

The Langmuir isotherm model refers to sorbate monolayer formation on the adsorbent surface with a homogeneous surface [53].

The Langmuir equation's linearized form is expressed as:

$$\frac{C_{eq}}{q_e} = \frac{1}{q_{max}b} + \frac{C_{eq}}{q_{max}} \quad (7)$$

where b (L/mg) is the adsorption constant of Langmuir associated with the sorption of free energy, and q_{max} (mg/g) is the maximum sorption capability of the algal biomass. The values of q_{max} and b can be estimated from the slope and intercept, respectively, of the C_{eq}/q_e against C_{eq} linear plot, as indicated in Figure 7A.

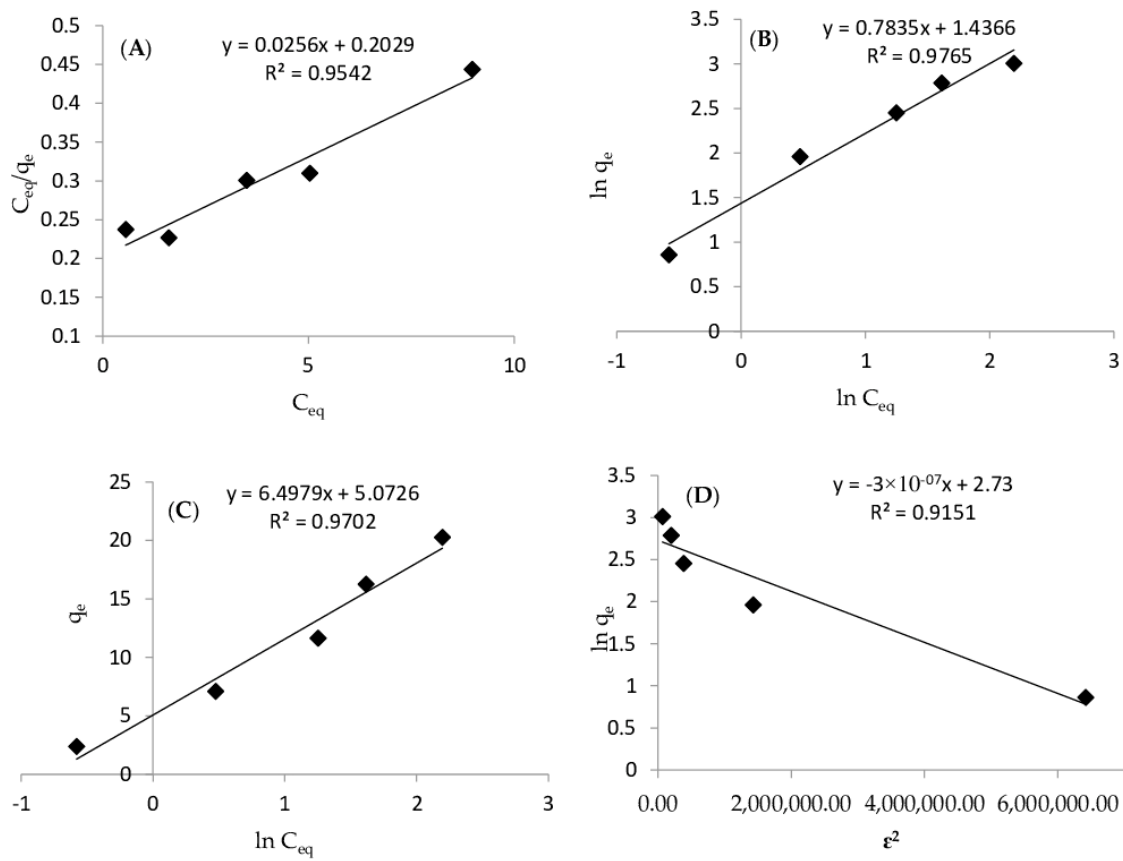


Figure 7. (A) Langmuir, (B) Freundlich, (C) Temkin, and (D) Dubinin and Radushkevich isotherm models for the biosorption of CV by *S. muticum* biomass.

The data indicates that the maximum adsorption capability of CV dye (q_{max}) on *S. muticum* biomass of 39.1 mg/g was accomplished with a biosorption constant b of 0.12 L/mg, as well as a high coefficient of determination value ($R^2 = 0.954$; Table 2) indicated that the process of CV dye biosorption suits the Langmuir isotherm model.

This means that the *S. muticum* biomass could be used for the removal of CV dye from aqueous solutions as a potential biosorbent.

A dimensionless separation factor (R_L) gives valuable facts about the sorption nature. The Equation can be found as follows:

$$R_L = \frac{1}{1 + bC_0} \quad (8)$$

where C_0 (mg/L): the initial concentration of the CV dye. R_L values suggest that the isothermal shapes are either favorable ($0 < R_L < 1$), unfavorable ($R_L > 1$), or linear ($R_L = 1$) [54]. The R_L values ranged from 0.09 to 0.33, suggesting a desirable process of biosorption.

Reversible and non-ideal sorption is defined by the Freundlich isotherm. It is not limited to monolayer forming and could be used in heterogeneous sites for multilayer sorption [55]. The Equation's linearized form of Freundlich model is found as follows:

$$\ln q_e = \ln K_f + \frac{1}{n} \ln C_{eq} \quad (9)$$

where K_f is the adsorption constant of Freundlich (mg/g), showing the magnitude capability of sorption, and n is the intensity of adsorption that is used for the description of the surface heterogeneity or sorption strength [18].

The values of n and K_f were deduced from the slope and intercept of the $\ln q_e$ against $\ln C_{eq}$ linear plot, respectively (Figure 7B).

The findings revealed that the adsorption constant (K_f) was 4.21 (mg/g) with a high-value R^2 (0.977), and the value of sorption intensity (n) was 1.27, indicating a higher CV dye/biosorbent interaction (Table 2). The multilayer biosorption processes were thus dominant, and the isothermal Freundlich model is well used for the description of CV dye biosorption by the biomass of *S. muticum*. Similar results were recorded for the CV dye biosorption onto *Rhizophora mucronata* stem barks [56] and the Congo red removal by *Cystoseira trinodis* [50]. The slight variation between the isotherms of Langmuir and Freundlich models in the values of R^2 indicated that both models were suitable for the biosorption of CV dye onto *S. muticum* biomass.

The Temkin isotherm model implies that the energy of adsorption for all molecules is decreased linearly rather than logarithmic with surface coverage, taking into account the adsorbate-adsorbent interaction effect [57]. The Equation's linearized form is expressed as:

$$q_e = B \ln A + B \ln C_{eq} \quad (10)$$

where B is a constant related to the energy of sorption, and A (L/mg) is Temkin isothermal constant (the constant of equilibrium binding associated with the maximum binding energy) and given by Equation (11):

$$B = \frac{RT}{b} \quad (11)$$

where T (K) is the absolute temperature (298.15), R is the gas constant (8314 J/mol K), and b (J/mol) is the sorption energy-related constant of the Temkin model.

The values of B and A were estimated by the plotting of q_e vs. $\ln C_{eq}$ from the slope (B) and intercept ($B \ln A$), respectively (Figure 7C; Table 2). A higher biosorbent-dye potential was revealed by the high Temkin isothermal constant ($A = 2.18$ L/mg). Moreover, the high value of the Temkin constant ($b = 381$ J/mol) showed a strong interaction between algal biomass and CV dye molecules [58]. The high value of the determination coefficient ($R^2 = 0.970$; Table 2) indicates that the Temkin isotherm model suits well with the CV dye biosorption onto the biomass of *S. muticum*.

The Dubinin–Radushkevich isotherm model is used for determining the mechanism of pore filling and assessment of the chemical or physical nature of the sorption process [59]. The isotherm of D–R model is found as follows:

$$\ln q_e = \ln q_0 - \beta \varepsilon^2 \quad (12)$$

where ε is the potential of Polanyi, β (mol²/J²) is the coefficient of activity correlated with the mean energy of adsorption, and q_0 (mg/g) is the maximal sorption capacity. From the intercept and slope of the plotting of $\ln q_e$ against ε^2 , the values β and q_0 were determined (Figure 7D). The value of ε has been calculated from the following Equation:

$$\varepsilon = RT \ln \left(1 + \frac{1}{C_{eq}} \right) \quad (13)$$

In order to explain the sorption type, whether physical ($E < 8$ kJ/mol) or chemical sorption ($E = 8–16$ kJ/mol), the model of D–R utilizes the mean sorption energy (E) [60]. It is calculated from Equation (14) as follows:

$$E = \sqrt{1/2\beta} \quad (14)$$

The value of the mean free adsorption energy of CV biosorption by *S. muticum* was more than 8 kJ/mol (12.9 kJ/mol; Table 2), suggesting chemisorption was involved in the process of adsorption. The high calculated R^2 value (0.915) indicates that the data of the CV dye biosorption by *S. muticum* were fitted by the D–R isotherm model.

3.5. Effect of Temperature and Thermodynamic Studies

The removal of CV dye was assessed for varied temperature values of 25, 35, and 45 °C under optimized conditions of 60 min contact time, 10 g/L algal dosage, 30 mg/L initial CV concentration, and pH 6. Figure 8A shows that the removal percentage of CV dye increased with increasing temperature. The increased biosorption may be a result of both the higher kinetic energy of the CV dye molecules and the increased activity of the adsorbent surface [61]. The enhanced mobility of dye molecules and the presence of pores on the algal surface may also possibly contribute to this effect. According to Rajasimman and Murugaiyan [62], the increased temperature causes dye molecules to diffuse faster on the surface and inside the pores of algal biomass.

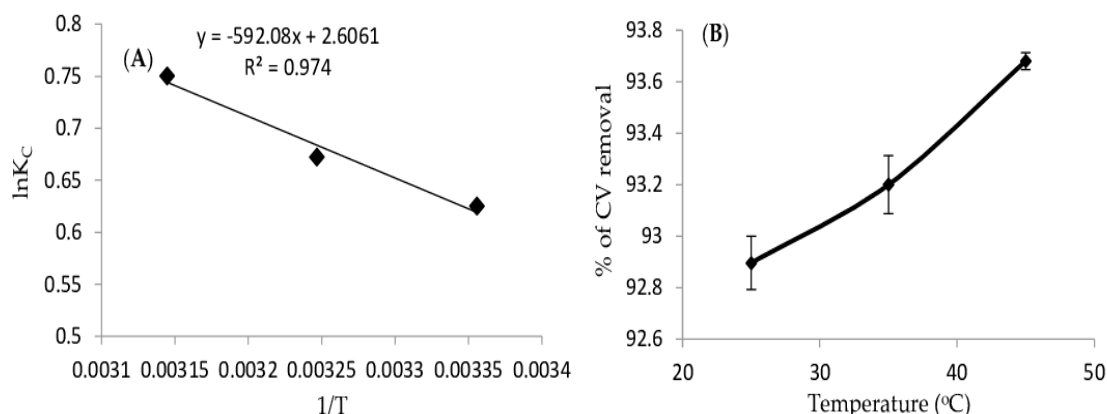


Figure 8. (A) Effect of temperature on the biosorption process of CV onto the *S. muticum* biomass, (B) Plot of $\ln K_C$ against $1/T$ for the biosorption of CV onto *S. muticum* biomass.

For achieving the thermodynamic parameters at optimal conditions of 60 min contact time, 10 g/L algal dose, 30 mg/L of initial concentration of CV dye, and pH of 6, the impact of different temperature values (25, 35 and 45 °C) on the adsorption process of CV dye by the *S. muticum* biomass was studied.

Thermodynamic parameters, including Gibbs free energy (ΔG^0), entropy change (ΔS^0), and enthalpy change (ΔH^0), may provide considerable details on the energy variations in the adsorption process of CV dye on the algal biomass. The following equations could be used to determine the thermodynamic parameters [63,64].

$$K_C = \frac{C_s}{C_{eq}} \quad (15)$$

$$\ln K_C = \frac{\Delta S^0}{R} - \frac{\Delta H^0}{RT} \quad (16)$$

$$\Delta G^0 = \Delta H^0 - T\Delta S^0 \quad (17)$$

where K_C is the distribution ratio of the adsorbed CV dye concentration (C_s) to the CV dye concentration in the solution (C_{eq}), the linear plot of $\ln K_C$ against $1/T$ produces the ΔS^0 and ΔH^0 values of the intercept and slope, respectively (Figure 8B).

The results in Table 3 showed that the values of ΔG^0 were negative, indicating that the biosorption process is spontaneous and that the energy required is given by the decrease in temperature. The positive value of enthalpy change, ΔH^0 (4.91 kJ/mol), verified that the biosorption of CV dye onto the *S. muticum* biomass was an endothermic process such that by raising the adsorbate-adsorbent system temperature, the biosorption efficiency of CV dye can be increased. The endothermic nature of biosorption was described in different studies. Jafari [65] stated an increase in CV and MB biosorption onto magnetic *Fucus vesiculosus* with a rise in temperature. Additionally, Fawzy [42] found that increasing the temperature from 298 to 318 °K increased the biosorption of Cu^{2+} ions by dried biomass of

Codium vermilara. The positive value of entropy change, ΔS° (0.022 kJ/mol), on the other hand, indicated an increase in randomness at the solid/solution interface by biosorption of CV dye onto *S. muticum* biomass [66].

Table 3. Thermodynamic parameters for the CV biosorption onto *S. muticum* biomass.

Temperature (K)	ΔG° (kJ/mol)	ΔH° (kJ/mol)	ΔS° (kJ/mol)	R^2
298	−1.54			
308	−1.72	4.91	0.022	0.974
318	−1.98			

3.6. Application in Real Wastewater Treatment

A biosorption experiment was performed on real wastewater obtained from agricultural wastewater at Wady Al-Arj, Taif, Saudi Arabia (21°19' N and 40°32' E, and altitude of 1591 m), where the temperature = 21.8 °C, pH = 8.92, total dissolved solids = 751.4 mg/L and conductivity = 1174 μ S/cm to test the efficacy of *S. muticum* as a biosorbent for the removal of crystal violet dye from agricultural effluents. Because the crystal violet concentration was low, a high quantity of CV was added to the wastewater to attain a final concentration of 30 mg/L.

The batch method was used to investigate the biosorption efficacy of crystal violet under optimal conditions (60 min contact time, 10 g/L algal dosage, and pH 6) using 100 mL of wastewater. The removal efficiency of crystal violet was found to be high, up to $91.81 \pm 1.58\%$, indicating that algal biomass could efficiently remove harmful dyes from wastewater.

3.7. Comparison of Crystal Violet Dye Biosorption Capacity with Other Sorbents

Table 4 compares the maximum biosorption capacity determined in this research to various sorbents examined in the literature for crystal violet dye removal. The maximum uptake capacity of CV dye by *S. muticum* in the current study was determined to be 39.1 mg g^{-1} , which was compared to q_{max} obtained from other studies on CV dye removal. The findings demonstrate the high capacity of *S. muticum* for crystal violet dye biosorption.

Table 4. The comparison of the maximum adsorption capacity of crystal violet by different sorbents.

Adsorbents	Biosorption Conditions		q_{max} (mg/g)	References
	Contact Time (min)	pH		
<i>Skeletonema costatum</i> diatom	120	3	10.77	[33]
<i>Rhizophora mucronata</i> stem-bark	60	7	1.18	[56]
Zeolite from bottom ash	10	6.5	17.6	[67]
Leaf biomass of <i>Calotropis procera</i>	60	-	4.14	[68]
Lignin-rich Isolate from Elephant Grass	30	-	24.99	[69]
Pineapple crown leaves	-	-	6.49	[70]
<i>Iridaea cordata</i> macroalga	90	7	36.5	[71]
<i>Gracilaria corticata</i> macroalga	-	8	28.9	[72]
<i>Laminaria japonica</i> macroalga	-	10	14.5	[73]
<i>Sargassum muticum</i>	60	6	39.1	Present study

3.8. Biosorption Mechanism

The cell walls of Brown algae contain a variety of functional groups, including amine, carboxyl, carbonyl, amino, hydroxyl, and sulfate, as indicated by the analysis of FT-IR, which are in charge of removing harmful substances from industrial wastewater [1].

In the sorbent/sorbate systems, the interactions of hydrogen bonding primarily occur between the hydrogen surface of $-\text{OH}$, $-\text{COOH}$, $-\text{NH}$, and CH_2 groups (which are considered as hydrogen donor groups) on the *S. muticum* surface and the nitrogen atom (H-acceptor group) of CV dye (dipole–dipole H-bonding). Additionally, it occurs between

the aromatic rings in the molecules of CV dye and the hydrogen donor groups of the algal biomass (Yoshida H-bonding). As an alternative method of CV dye biosorption, use the aromatic rings of the CV dye as the electron acceptor and the oxygen groups of the algal surface as the electron donor; these interactions of hydrogen-bonding in this mechanism are known as n - π interactions (electron acceptor-donor interactions). The binding of CV molecules is significantly influenced by the functional groups formed from oxygen (such as COOH and OH) that are present on the sorbent surface.

The mechanism of CV dye biosorption can also take place via an ion exchange and electrostatic interaction process because the biosorbent surface is negatively charged at $\text{pH} \leq 6$; this simplifies the binding of the algal surface to the positively charged molecules of CV dye. The ion exchange mechanism can take place by exchanging the sodium, magnesium, and calcium ions found on the algal cell wall with the ions from the CV dye [74]. In addition, the electrostatic interaction occurs between negatively charged functional groups, like $-\text{COOH}$, $-\text{OH}$, and $-\text{NH}$, found on the surface of biosorbent and the positively charged CV dye ions. Therefore, it can be inferred that hydrogen bonding, ion exchange, and electrostatic interaction mechanisms can all contribute to biosorb CV dye onto the biomass of *S. muticum*.

4. Conclusions

It was clearly seen in the present study that *S. muticum* could effectively be used as a low-cost biosorbent for the removal of crystal violet dye. Several factors have been examined, such as contact time, algal dosage, initial concentration of the CV dye, and pH. In modeling the process of biosorption, four isotherms and kinetic equations were used. The isotherm fits the models of Langmuir, Freundlich, Dubinin-Radushkevich, and Temkin, while the kinetics fit the pseudo-second-order and Elovich models with a higher determination coefficient. To assess the progress rate of the CV biosorption process, the model of intraparticle diffusion has been found. This revealed that smaller particles had a greater impact on the boundary layer. Thermodynamic parameters demonstrated endothermic, randomness, and spontaneous biosorption of CV and the mechanism of biosorption. Ultimately, the analysis of FTIR verified that the major groups involved in the biosorption process of CV dye were the sulfate, carbonyl, amine, and hydroxyl groups. Moreover, the formation of hydrogen bonds, electrostatic interaction, and ion exchange all played a role in the biosorption mechanism of CV dye onto the algal biomass. As a result, *S. muticum* was found to be a good low-cost biosorbent for removing textile toxic dye from aqueous solutions and real wastewater via the adsorption process.

Supplementary Materials: The following supporting information can be downloaded at: <https://www.mdpi.com/article/10.3390/su152015064/s1>, Figure S1. pH_{ZPC} of *S. muticum* biomass.

Author Contributions: Conceptualization, writing—original draft preparation, investigation, software, methodology, validation, visualization and formal analysis, M.A.F.; writing—review and editing, supervision, validation, and visualization, A.S.A.; investigation, supervision, software, validation, writing—review and editing, and visualization S.H.A.H. and I.R.A.-R.; writing—review and editing and funding acquisition, A.H.A., A.A.A. and M.K. All authors have read and agreed to the published version of the manuscript.

Funding: This research was funded by Princess Nourah bint Abdulrahman University Researchers Supporting Project number (PNURSP2023R357), Princess Nourah bint Abdulrahman University, Riyadh, Saudi Arabia.

Institutional Review Board Statement: Not applicable.

Informed Consent Statement: Not applicable.

Data Availability Statement: Not applicable.

Acknowledgments: Princess Nourah bint Abdulrahman University Researchers Supporting Project number (PNURSP2023R357), Princess Nourah bint Abdulrahman University, Riyadh, Saudi Arabia.

Conflicts of Interest: The authors declare no conflict of interest.

References

1. Al-Zaban, M.I.; Alharbi, N.K.; Albarakaty, F.M.; Alharthi, S.; Hassan, S.H.; Fawzy, M.A. Experimental Modeling Investigations on the Biosorption of Methyl Violet 2B Dye by the Brown Seaweed *Cystoseira tamariscifolia*. *Sustainability* **2022**, *14*, 5285. [\[CrossRef\]](#)
2. Vergis, B.R.; Krishna, R.H.; Kottam, N.; Nagabhushana, B.M.; Sharath, R.; Darukaprasad, B. Removal of malachite green from aqueous solution by magnetic CuFe₂O₄ nano-adsorbent synthesized by one pot solution combustion method. *J. Nanostruct. Chem.* **2018**, *8*, 1–12. [\[CrossRef\]](#)
3. Hsini, A.; Essecri, A.; Aarab, N.; Laabd, M.; Ait Addi, A.; Lakhmiri, R.; Albourine, A. Elaboration of novel polyaniline@Almond shell biocomposite for effective removal of hexavalent chromium ions and Orange G dye from aqueous solutions. *Environ. Sci. Pollut. Res.* **2020**, *27*, 15245–15258. [\[CrossRef\]](#) [\[PubMed\]](#)
4. Koli, P.B.; Kapadnis, K.H.; Deshpande, U.G.; Patil, M.R. Fabrication and characterization of pure and modified Co₃O₄ nanocatalyst and their application for photocatalytic degradation of eosine blue dye: A comparative study. *J. Nanostruct. Chem.* **2018**, *8*, 453–463. [\[CrossRef\]](#)
5. Mittal, A.; Mittal, J.; Malviya, A.; Kaur, D.; Gupta, V.K. Adsorption of hazardous dye crystal violet from wastewater by waste materials. *J. Colloid Inter. Sci.* **2010**, *343*, 463–473. [\[CrossRef\]](#)
6. Jana, S.; Ray, J.; Mondal, B.; Pradhan, S.S.; Tripathy, T. pH responsive adsorption/desorption studies of organic dyes from their aqueous solutions by katira gum-cl-poly (acrylic acid-co-N-vinyl imidazole) hydrogel. *Colloid Surface A* **2018**, *553*, 472–486. [\[CrossRef\]](#)
7. Ghaedi, M.; Shojaeipour, E.; Ghaedi, A.M.; Sahraei, R. Isotherm and kinetics study of malachite green adsorption onto copper nanowires loaded on activated carbon: Artificial neural network modeling and genetic algorithm optimization, *Spectrochim. Acta A Mol. Biomol. Spectrosc.* **2015**, *142*, 135–149. [\[CrossRef\]](#)
8. Moghaddam, S.S.; Moghaddam, M.A.; Arami, M. Coagulation/flocculation process for dye removal using sludge from water treatment plant: Optimization through response surface methodology. *J. Hazard. Mater.* **2010**, *175*, 651–657. [\[CrossRef\]](#)
9. Luo, X.P.; Fu, S.Y.; Du, Y.M.; Guo, J.Z.; Li, B. Adsorption of methylene blue and malachite green from aqueous solution by sulfonic acid group modified MIL-101. *Micropor. Mesopor. Mat.* **2017**, *237*, 268–274. [\[CrossRef\]](#)
10. Kaushik, P.; Malik, A. Fungal dye decolourization: Recent advances and future potential. *Environ. Int.* **2009**, *35*, 127–141. [\[CrossRef\]](#)
11. Daneshvar, E.; Vazirzadeh, A.; Niazi, A.; Kousha, M.; Naushad, M.; Bhatnagar, A. Desorption of Methylene blue dye from brown macroalga: Effects of operating parameters, isotherm study and kinetic modeling. *J. Clean. Prod.* **2017**, *152*, 443–453. [\[CrossRef\]](#)
12. Goel, N.K.; Kumar, V.; Misra, N.; Varshney, L. Cellulose based cationic adsorbent fabricated via radiation grafting process for treatment of dyes waste water. *Carbohydr. Polym.* **2015**, *132*, 444–451. [\[CrossRef\]](#)
13. Saroj, S.; Singh, S.V.; Mohan, D. Removal of colour (Direct Blue 199) from carpet industry wastewater using different biosorbents (maize cob, citrus peel and rice husk). *Arabian J. Sci. Eng.* **2015**, *40*, 1553–1564. [\[CrossRef\]](#)
14. Cengiz, S.; Cavas, L. Removal of methylene blue by invasive marine seaweed: *Caulerpa racemosa* var. *cylindracea*. *Bioresour. Technol.* **2008**, *99*, 2357–2363. [\[CrossRef\]](#) [\[PubMed\]](#)
15. Wang, L.; Li, Q.; Wang, A.Q. Adsorption of cationic dye on N,O-carboxymethyl-chitosan from aqueous solutions: Equilibrium, kinetics, and adsorption mechanism. *Polym. Bull.* **2010**, *65*, 961–975. [\[CrossRef\]](#)
16. Abdallah, R.; Taha, S. Biosorption of methylene blue from aqueous solution by nonviable *Aspergillus fumigatus*. *Chem. Eng. J.* **2012**, *195*, 69–76. [\[CrossRef\]](#)
17. Balci, B.; Erkurt, F.E. Adsorption of reactive dye from aqueous solution and synthetic dye bath wastewater by *Eucalyptus* bark/magnetite composite. *Water Sci. Technol.* **2016**, *74*, 1386–1397. [\[CrossRef\]](#)
18. Fawzy, M.A.; Gomaa, M. Low-cost biosorption of Methylene Blue and Congo Red from single and binary systems using *Sargassum latifolium* biorefinery waste/wastepaper xerogel: An optimization and modeling study. *J. Appl. Phycol.* **2021**, *33*, 675–691. [\[CrossRef\]](#)
19. Kousha, M.; Daneshvar, E.; Sohrabi, M.S.; Jokar, M.; Bhatnagar, A. Adsorption of acid orange II dye by raw and chemically modified brown macroalga *Stoechospermum marginatum*. *Chem. Eng. J.* **2012**, *192*, 67–76. [\[CrossRef\]](#)
20. Anastopoulos, I.; Kyzas, G.Z. Progress in batch biosorption of heavy metals onto algae. *J. Mol. Liq.* **2015**, *209*, 77–86. [\[CrossRef\]](#)
21. Tabaraki, R.; Sadeghinejad, N. Biosorption of six basic and acidic dyes on brown alga *Sargassum ilicifolium*: Optimization, kinetic and isotherm studies. *Water Sci. Technol.* **2017**, *75*, 2631–2638. [\[CrossRef\]](#) [\[PubMed\]](#)
22. Wang, X.S.; Zhou, Y.; Jiang, Y. Evaluation of marine brown *Laminaria japonica* algae as a low-cost adsorbent for the removal of malachite green dye from aqueous solution. *Adsorp. Sci. Technol.* **2009**, *27*, 537–547. [\[CrossRef\]](#)
23. Esmaeli, A.; Jokar, M.; Kousha, M.; Daneshvar, E.; Zilouei, H.; Karimi, K. Acidic dye wastewater treatment onto a marine macroalga, *Nizamuddina zanardini* (Phylum: Ochrophyta). *Chem. Eng. J.* **2013**, *217*, 329–336. [\[CrossRef\]](#)
24. Liang, J.; Xia, J.; Long, J. Biosorption of methylene blue by nonliving biomass of the brown macroalga *Sargassum hemiphyllum*. *Water Sci. Technol.* **2017**, *76*, 1574–1583. [\[CrossRef\]](#) [\[PubMed\]](#)
25. Alharbi, N.K.; Al-Zaban, M.I.; Albarakaty, F.M.; Abdelwahab, S.F.; Hassan, S.H.; Fawzy, M.A. Kinetic, isotherm and thermodynamic aspects of Zn²⁺ biosorption by *Spirulina platensis*: Optimization of process variables by response surface methodology. *Life* **2022**, *12*, 585. [\[CrossRef\]](#)

26. Omar, H.; El-Gendy, A.; Al-Ahmary, K. Bioremoval of toxic dye by using different marine macroalgae. *Turkish J. Bot.* **2018**, *42*, 15–27. [[CrossRef](#)]
27. Vijayaraghavana, G.; Shanthakumar, S. Removal of Crystal violet dye in textile effluent by coagulation using algal alginate from brown algae *Sargassum* sp. In Proceedings of the First International Conference on Recent Trends in Clean Technologies for Sustainable Environment (CTSE-2019), Chennai, India, 26–27 September 2019; Volume 26, p. 27.
28. Keshtkar, M.; Dobaradaran, S.; Keshmiri, S.; Ramavandi, B.; Arfaeina, H.; Ghaedi, H. Effective parameters, equilibrium, and kinetics of fluoride adsorption on *Prosopis cineraria* and *Syzygium cumini* Leaves. *Environ. Prog. Sustain. Energy* **2019**, *38* (Suppl. S1), S429–S440. [[CrossRef](#)]
29. El Atouani, S.; Bentiss, F.; Reani, A.; Zrid, R.; Belattmania, Z.; Pereira, L.; Mortadi, A.; Cherkaoui, O.; Sabour, B. The invasive brown seaweed *Sargassum muticum* as new resource for alginate in Morocco: Spectroscopic and rheological characterization: *S. muticum* as an alginophyt in Morocco. *Phycol. Res.* **2016**, *64*, 185–193. [[CrossRef](#)]
30. Pennesi, C.; Rindi, F.; Totti, C.; Beolchini, F. Marine Macrophytes: Biosorbents. In *Springer Handbook of Marine Biotechnology*; Springer: Berlin/Heidelberg, Germany, 2015; pp. 597–610.
31. Marais, M.F.; Joseleau, J.P. A fucoidan fraction from *Ascophyllum nodosum*. *Carbohydr. Res.* **2001**, *336*, 155–159. [[CrossRef](#)]
32. Kumar, R.; Ahmad, R. Biosorption of hazardous crystal violet dye from aqueous solution onto treated ginger waste (TGW). *Desalination* **2011**, *265*, 112–118. [[CrossRef](#)]
33. Ashour, M.; Alprol, A.E.; Khedawy, M.; Abualnaja, K.M.; Mansour, A.T. Equilibrium and Kinetic Modeling of Crystal Violet Dye Adsorption by a Marine Diatom, *Skeletonema costatum*. *Materials* **2022**, *15*, 6375. [[CrossRef](#)] [[PubMed](#)]
34. Shao, H.; Li, Y.; Zheng, L.; Chen, T.; Liu, J. Removal of methylene blue by chemically modified defatted brown algae *Laminaria japonica*. *J. Taiwan Inst. Chem. Eng.* **2017**, *80*, 525–532. [[CrossRef](#)]
35. Maurya, R.; Ghosh, T.; Paliwal, C.; Shrivastav, A.; Chokshi, K.; Pancha, I.; Ghosh, A.; Mishra, S. Biosorption of methylene blue by de-oiled algal biomass: Equilibrium, kinetics and artificial neural network modelling. *PLoS ONE* **2014**, *9*, e109545. [[CrossRef](#)]
36. Jayaraj, R.; Mohan, M.C.; Prasath, P.M.D.; Khan, T.H. Malachite green dye removal using the seaweed *Enteromorpha*. *E-J. Chem.* **2011**, *8*, 649–656. [[CrossRef](#)]
37. Aditiya, I.; Al Kausar, R. Production of a *Spirulina* sp. algae hybrid with a silica matrix as an effective adsorbent to absorb crystal violet and methylene blue in a solution. *Sustain. Environ. Res.* **2019**, *29*, 1–11.
38. Daneshvar, E.; Kousha, M.; Jokar, M.; Koutahzadeh, N.; Guibal, E. Acidic dye biosorption onto marine brown macroalgae: Isotherms, kinetic and thermodynamic studies. *Chem. Eng. J.* **2012**, *204*, 225–234. [[CrossRef](#)]
39. Gupta, V.K.; Rastogi, A. Biosorption of hexavalent chromium by raw and acid treated green alga *Oedogonium hatei* from aqueous solutions. *J. Hazard. Mater.* **2009**, *163*, 396–402. [[CrossRef](#)]
40. Badmus, M.A.O.; Audu, T.O.K.; Anyata, B.U. Removal of lead ion from industrial wastewater by activated carbon prepared from Periwinkle Shells (*Typanotonus fuscatus*). *Turkish J. Eng. Environ. Sci.* **2007**, *31*, 251–263.
41. Chakraborty, S.; Chowdhury, S.; Saha, P.D. Insight into biosorption equilibrium, kinetics and thermodynamics of crystal violet onto *Ananas comosus* (pineapple) leaf powder. *Appl. Water Sci.* **2012**, *2*, 135–141. [[CrossRef](#)]
42. Fawzy, M.A. Biosorption of copper ions from aqueous solution by *Codium vermilara*: Optimization, kinetic, isotherm and thermodynamic studies. *Adv. Powder Technol.* **2020**, *31*, 3724–3735. [[CrossRef](#)]
43. Nemr, A.E.; El-Sikaily, A.; Khaled, A.; Abdelwahab, O. Removal of toxic chromium from aqueous solution, wastewater and saline water by marine red alga *Pterocladia capillacea* and its activated carbon. *Arabian J. Chem.* **2015**, *8*, 105–117. [[CrossRef](#)]
44. Rivera-Utrilla, J.; Bautista-Toledo, I.; Ferro-García, M.A.; Moreno-Castilla, C. Activated carbon surface modifications by adsorption of bacteria and their effect on aqueous lead adsorption. *J. Chem. Technol. Biotechnol.* **2001**, *76*, 1209–1215. [[CrossRef](#)]
45. Ncibi, M.C.; Ben Hamissa, A.M.; Fathallah, A.; Kortas, M.H.; Baklouti, T.; Mahjoub, B.; Seffen, M. Biosorptive uptake of methylene blue using Mediterranean green alga *Enteromorpha* spp. *J. Hazard. Mater.* **2009**, *170*, 1050–1055. [[CrossRef](#)]
46. Lagergren, S. Zur theorie der sogenannten adsorption gelöster stoffe, Kungliga Svenska Vetenskapsakademiens. *Handlingar* **1898**, *24*, 1–39.
47. Ho, Y.S.; McKay, G. Sorption of dye from aqueous solution by peat. *Chem. Eng. J.* **1998**, *70*, 115–124. [[CrossRef](#)]
48. Wu, F.C.; Tseng, R.L.; Juang, R.S. Characteristics of Elovich equation used for the analysis of adsorption kinetics in dyechitosan systems. *Chem. Eng. J.* **2009**, *150*, 366–373. [[CrossRef](#)]
49. Weber, W.J.; Morris, J.C. Kinetics of adsorption on carbon from solution. *J. Sanit. Eng. Div. Am. Soc. Civil Eng.* **1963**, *89*, 31–60. [[CrossRef](#)]
50. Fawzy, M.A.; Goma, M. Use of algal biorefinery waste and waste office paper in the development of xerogels: A low cost and eco-friendly biosorbent for the effective removal of congo red and Fe (II) from aqueous solutions. *J. Environ. Manag.* **2020**, *262*, 110380. [[CrossRef](#)]
51. Benavente, M.; Moreno, L.; Martinez, J. Sorption of heavy metals from gold mining wastewater using chitosan. *J. Taiwan Inst. Chem. Eng.* **2011**, *42*, 976–998. [[CrossRef](#)]
52. Benally, C.; Messele, S.A.; El-Din, M.G. Adsorption of organic matter in oil sands process water (OSPW) by carbon xerogel. *Water Res.* **2019**, *154*, 402–411. [[CrossRef](#)]
53. Toor, M.; Jin, B. Adsorption characteristics, isotherm, kinetics and diffusion of modified natural bentonite for removing diazo dye. *Chem. Eng. J.* **2012**, *187*, 79–88. [[CrossRef](#)]

54. Cobas, M.; Sanromán, M.; Pazos, M. Box–Behnken methodology for Cr (VI) and leather dyes removal by an eco-friendly biosorbent: *F. vesiculosus*. *Bioresour. Technol.* **2014**, *160*, 166–174. [[CrossRef](#)] [[PubMed](#)]
55. Foo, K.Y.; Hameed, B.H. Insights into the modeling of adsorption isotherm systems. *Chem. Eng. J.* **2010**, *156*, 2–10. [[CrossRef](#)]
56. Oloo, C.M.; Onyari, J.M.; Wanyonyi, W.C.; Wabomba, J.N.; Muinde, V.M. Adsorptive removal of hazardous crystal violet dye from aqueous solution using *Rhizophora mucronata* stem-barks: Equilibrium and kinetics studies. *Environ. Chem. Ecotoxicol.* **2020**, *2*, 64–72. [[CrossRef](#)]
57. Yurtsever, M.; Sengil, I.A. Biosorption of Pb(II) ions by modified quebracho tannin resin. *J. Hazard. Mater.* **2009**, *163*, 58–64. [[CrossRef](#)]
58. Shahmohammadi-Kalalagh, S.; Babazadeh, H.; Nazemiand, A.H.; Manshouri, M. Isotherm and kinetic studies on adsorption of Pb, Zn and Cu by kaolinite. *Caspian J. Environ. Sci.* **2011**, *9*, 243–255.
59. Chakraborty, S.; Chowdhury, S.; Saha, P.D. Adsorption of crystal violet from aqueous solution onto NaOH-modified rice husk. *Carbohydr. Polym.* **2011**, *86*, 1533–1541. [[CrossRef](#)]
60. Fawzy, M.A.; Hifney, A.F.; Adam, M.S.; Al-Badaani, A.A. Biosorption of cobalt and its effect on growth and metabolites of *Synechocystis pevalekii* and *Scenedesmus bernardii*: Isothermal analysis. *Environ. Technol. Innov.* **2020**, *19*, 100953. [[CrossRef](#)]
61. Motik, C.; Chegdani, F.; Blaghen, M. The biosorption potential of Plocamium cartilagineum algal biomass for the elimination of the synthetic dye Cibacron Blue. *Aquac. Conserv. Legis.* **2022**, *15*, 544–556.
62. Rajasimman, M.; Murugaiyan, K. Optimization of process variables for the biosorption of chromium using *Hypnea valentiae*. *Nova Biotechnol.* **2010**, *10*, 107–115. [[CrossRef](#)]
63. Rajabi, M.; Mahanpoor, K.; Moradi, O. Preparation of PMMA/GO and PMMA/GO-Fe₃O₄ nanocomposites for malachite green dye adsorption: Kinetic and thermodynamic studies. *Compos. Part B Eng.* **2019**, *167*, 544–555. [[CrossRef](#)]
64. Khosravi, R.; Moussavi, G.; Ghaneian, M.T.; Ehrampoush, M.H.; Barikbin, B.; Ebrahimi, A.A.; Sharifzadeh, G. Chromium adsorption from aqueous solution using novel green nanocomposite: Adsorbent characterization, isotherm, kinetic and thermodynamic investigation. *J. Mol. Liq.* **2018**, *256*, 163–174. [[CrossRef](#)]
65. Jafari, H.; Mahdavinia, G.R.; Kazemi, B.; Javanshir, S.; Alinavaz, S. Basic dyes removal by adsorption process using magnetic *Fucus vesiculosus* (brown algae). *J. Water Environ. Nanotechnol.* **2020**, *5*, 256–269.
66. Fawzy, M.A.; Alharthi, S. Cellular responses and phenol bioremoval by green alga *Scenedesmus abundans*: Equilibrium, kinetic and thermodynamic studies. *Environ. Technol. Innov.* **2021**, *22*, 101463. [[CrossRef](#)]
67. Bertolini, T.C.R.; Izidoro, J.C.; Magdalena, C.P.; Fungaro, D.A. Adsorption of crystal violet dye from aqueous solution onto zeolites from coal fly and bottom ashes. *Orbital Electron. J. Chem.* **2013**, *5*, 179–191.
68. Ali, H.; Muhammad, S.K. Biosorption of crystal violet from water on leaf biomass of *Calotropis procera*. *J. Environ. Sci. Technol.* **2008**, *1*, 143–150. [[CrossRef](#)]
69. Menkiti, M.; Aniagor, C.; Agu, C.; Ugonabo, V. Effective adsorption of crystal violet dye from an aqueous solution using lignin-rich isolate from elephant grass. *Water Conserv. Sci. Eng.* **2018**, *3*, 33–46. [[CrossRef](#)]
70. Nieva, A.D.; Avena, L.G.S.; Pascual, M.A.M.; Pamintuan, K.R.S. Characterization of powdered pineapple (*Ananas comosus*) crown leaves as adsorbent for crystal violet in aqueous solutions. In *IOP Conference Series: Earth and Environmental Science, 2020 2nd International Conference on Resources and Environment Sciences, 5–7 June 2020, Kasetsart University, Bangkok, Thailand, 2020*; IOP Publishing: Bristol, UK, 2020; Volume 563, p. 012010. [[CrossRef](#)]
71. Escudero, L.B.; Smichowski, P.N.; Dotto, G.L. Macroalgae of *Iridaea cordata* as an efficient biosorbent to remove hazardous cationic dyes from aqueous solutions. *Water Sci. Technol.* **2017**, *76*, 3379–3391. [[CrossRef](#)]
72. Vijayaraghavan, J.; Bhagavathi Pushpa, T.; Sardhar Basha, S.J.; Jegan, J. Isotherm, kinetics and mechanistic studies of methylene blue biosorption onto red seaweed *Gracilaria corticata*. *Desalin. Water Treat.* **2016**, *57*, 13540–13548. [[CrossRef](#)]
73. Wang, X.S.; Liu, X.; Wen, L.; Zhou, Y.; Jiang, Y.; Li, Z. Comparison of basic dye crystal violet removal from aqueous solution by low-cost biosorbents. *Sep. Sci. Technol.* **2008**, *43*, 3712–3731. [[CrossRef](#)]
74. Shi, W.; Xia, M.; Wang, F.; Dong, L.; Zhu, S. Efficient absorption properties of surface grafted HEDP-HAP composites for Pb²⁺ and Cu²⁺: Experimental study and visualization study of interaction based on Becke surface analysis and independent gradient model. *J. Hazard. Mater.* **2021**, *401*, 123748. [[CrossRef](#)] [[PubMed](#)]

Disclaimer/Publisher’s Note: The statements, opinions and data contained in all publications are solely those of the individual author(s) and contributor(s) and not of MDPI and/or the editor(s). MDPI and/or the editor(s) disclaim responsibility for any injury to people or property resulting from any ideas, methods, instructions or products referred to in the content.